HHS Public Access

Author manuscript

Ann Biomed Eng. Author manuscript; available in PMC 2018 August 01.

Published in final edited form as:

Ann Biomed Eng. 2017 August ; 45(8): 2036–2047. doi:10.1007/s10439-017-1841-5.

Influence of inherent mechanophenotype on competitive cellular adherence

Manisha K. Shah[1], **Iris H. Garcia-Pak**[1], and **Eric M. Darling**[1,2,3,4]

[1]Center for Biomedical Engineering, Brown University, Rhode Island, USA

[2]Department of Molecular Pharmacology, Physiology, and Biotechnology, Brown University, Rhode Island, USA

[3]Department of Orthopaedics, Brown University, Rhode Island, USA

[4]School of Engineering, Brown University, Rhode Island, USA

Abstract

Understanding the role of mechanophenotype in competitive adherence of cells to other cells versus underlying substrates can inform such processes as tissue development, cancer progression, and wound healing. This study investigated how mechanophenotype, defined by whole-cell, elastic/viscoelastic properties for the perinuclear region, and cellular assembly are intertwined through the mechanosensing process. Atomic force microscopy was used to characterize the temporal elastic/viscoelastic properties of individual and assembled fibroblasts grown on substrates with elastic moduli above, below, or similar to whole-cell mechanophenotypes measured for three, genetically modified cell lines. All cells were at their most compliant immediately after plating but transitioned to distinct, stiffer mechanophenotypes by Day 1 after acclimation. This mechanical state, and cellular assembly/morphology, did not change significantly over the following three days of testing, regardless of substrate compliance or cellular organization (multi-cell nodules/plaques or single cells). Interestingly, cells formed 3D nodules when attached to substrates with elastic moduli less than their own but spread readily on substrates with moduli equal to or greater than their own, suggesting a preference to adhere to the stiffest surface sensed (substrate or cell). This suggests that inherent mechanophenotype plays a role as a competing surface during microenvironment mechanosensing and subsequent cell-cell-substrate organization.

Corresponding Author: Eric M. Darling, Brown University, 175 Meeting Street, Box G-B397, Providence, RI 02912, Phone: 401-863-6807, Fax: 401-863-7595, Eric_Darling@brown.edu.

Author Contributions

M.K.S. and E.M.D. designed the study, analyzed data, and wrote the manuscript. M.K.S. performed all AFM experiments and all experiments with non-transfected and transfected WI-38 cells lines. I.H.G.-P performed MG-63 and SH-SY5Y cellular assembly experiments. All authors gave final approval for publication.

Conflict of Interest

Manisha K. Shah, Iris H. Garcia-Pak, and Eric M. Darling declare that they have no conflicts of interest.

Data Accessibility

AFM and nodule quantification data can be downloaded from 10.6084/m9.figshare.4341887.

Keywords

mechanosensing; atomic force microscopy; nodule; plaque; elastic/viscoelastic properties; cellular assembly

Introduction

Mechanophenotype, which can be characterized using whole-cell, elastic and viscoelastic properties, has emerged as a viable biomarker and descriptor of cellular function and fate.[6–8,33] Changes in cellular mechanophenotype have been observed in different cell states, such as stem cell pluripotency/differentiation, cancer invasion, and cytoskeletal disruption or rearrangement.[6,9,15,20] Cells generate specific phenotypic responses to stimulatory factors in the cellular microenvironment, including an intricate combination of soluble and insoluble signaling molecules, physical stimuli, and cell-matrix and cell-cell interactions.[3,19] Previous studies have demonstrated how the extracellular environment drastically shapes cell behaviors. However, intrinsic properties of the cell, specifically mechanophenotype, have typically been overlooked but are invariably important to cell function (e.g., proliferation, self-renewal, differentiation, apoptosis, etc.).[10,11,31] We hypothesize that mechanophenotype will play a role in how a cell responds to its physical microenvironment, influencing the process of multicellular organization when in the presence of physiologically compliant surfaces.

Cellular assembly, defined by 2D and/or 3D cellular organization, is influenced by interactions between cells and substrates as well as between cells and other cells. While substantial effort over the past decade has been devoted towards understanding the effects of substrate compliance on cell behavior, the role of cellular mechanophenotype in cell-cell and cell-substrate interactions is not clearly understood.[12,23] Cells typically display a more rounded morphology and tend to aggregate on softer substrates, whereas cells attach and spread to a greater extent on stiffer substrates, with the latter also being dependent on the type and density of extracellular matrix (ECM) ligand coating.[14,23] Cellular mechanosensing of the microenvironment is linked to inherent mechanophenotype through cytoskeletal components, including focal adhesions, integrins, and cadherins.[28,32,35] Studies by Guo et al. and Gilchrist et al. both report formation of tissue-like aggregates on compliant substrates, observed across a range of cell types that included fibroblasts, epithelial cells, and nucleus pulposus cells, postulating that cells gain the most tension from cell-cell interactions compared to cell-substrate interactions.[14,16,24] The adhesion complexes formed through focal adhesions, integrins, and cadherins begin with actin polymerization and organization, followed by activation of myosin-II contractility that allows cells to migrate to regions of higher stiffness.[16,21,24] While this concept, known as durotaxis, has been extensively studied to understand the role of underlying substrates in cellular migration and adherence, little has been done in relation to cell-cell interactions. Understanding mechanophenotype in the context of cellular assembly could give rise to more effective tissue-specific constructs where appropriate cell-cell and cell-substrate interactions can develop.

The goal of this study was to (1) investigate the stability of inherent cellular mechanophenotype with respect to time and the compliance of the underlying substrate and (2) determine whether mechanophenotype can influence cellular adhesion and assembly when cells are grown on gels of known, physiologic elasticity. Human lung fibroblasts were mechanically characterized using atomic force microscopy (AFM) during four days of culture on collagen 1 (COL 1)-coated polyacrylamide (PAAm) gels to assess if and when mechanophenotype reached a state of equilibrium. Fibroblasts were transfected with three plasmids to create mechanically distinct cell lines: (1) GFP (control plasmid), (2) dnRhoA (to disrupt cytoskeletal regulation) and (3) β-Actin (to increase actin synthesis). The behavior of these stably transfected cell lines was then investigated when cells were grown on gels with stiffness above, below, and matching their whole-cell, elastic moduli. Changes in cellular mechanical properties and organizational phenotypes were assessed in relation to the mechanophenotype of the cell. We hypothesized that cells would maintain an inherent, internal mechanophenotype regardless of substrate stiffness. Additionally, cells would spread and attach more readily on substrates with elastic moduli equal to or greater than their own and that cells would compete to find and adhere to the stiffest surface sensed (substrate or cell).

Materials and Methods

Cell Culture

WI-38 VA-13 subline 2RA (WI-38, human lung fibroblasts, purchased from ATCC, #CCL-75.1) were expanded and maintained in phenol red-free MEM (CellGro, Corning) supplemented with 10% (volume/volume, v/v) FBS (Calsson Labs, lot #08142019 and #08152003), 1% (v/v) penicillin/streptomycin (Hyclone, GE Healthcare), 2 mM Glutamax (Hyclone, GE Healthcare), and 1 mM sodium pyruvate (Thermo Fisher Scientific). Cells were maintained in humidified incubators at 37° C, 5% CO_2 and passaged at 60–80% confluence using 0.25% trypsin-EDTA (Hyclone, GE Healthcare). MG-63 (osteosarcoma) and SH-SY5Y (neuroblastoma) cell lines were also used to confirm cell-cell-substrate assemblies and mechanical properties. The methodology and results for these additional experiments involving MG-63 and SH-SY5Y cells is shown in electronic supplementary text.

Development of Stable Cell Lines

WI-38 cells were plated in 96 well plates at 25,000 cells/well. After 24 hours, cells were transfected using NanoJuice™ Transfection Reagent (Novagen) according to product literature. Cells were transfected with one of three plasmids: pAcGFP1-Actin (β-Actin, #632453, Clontech), pcDNA3-EGFP-RhoA-T19N (dnRhoA, a gift from Gary Bokoch, #12967, Addgene), and pEmGFP-N1 (GFP, a gift from L. E. O. Darling, Wellesley College). Once cells reached 80–90% confluence post-transfection, cells were trypsinized and re-plated at low densities in 6-well plates in WI-38 culture media supplemented with 400 μg/mL Geneticin. After 4–7 days, when positively transfected colonies were visible (based on GFP fluorescence), 3–5 colonies were picked and expanded under antibiotic conditions. Colonies were grown and developed into stable cell lines in the presence of antibiotics.

Gel Fabrication and Functionalization

Polyacrylamide (PAAm) gels of three different stiffnesses were fabricated to be lower than, equal to, or greater than the stiffness of the transfected cell lines (0.3, 0.5, 1.4 kPa). Mechanical properties of the gels were modulated by using 3% acrylamide (#161-0140, Bio-Rad) with varying concentrations of bis-acrylamide (0.05, 0.07, and 0.2%, #161-0142, Bio-Rad) in phosphate buffered saline based on previously published protocols.[34] Gels were polymerized using 10% (weight/volume, w/v) ammonium persulfate (#BP179, Thermo Fisher Scientific) and 1.5% (v/v) tetramethylethylenediamine (#BP150, Thermo Fisher Scientific). 60 μl of the final PAAm solution was placed between a hydrophilic glass coverslip prepared using 0.5% (v/v) 3-aminopropyl-trimethoxysilane (#313251000, Acros Organics) and 0.5% (v/v) glutaraldehyde (#A17876, Alfa Aesar) and a hydrophobic glass slide prepared using 0.5% acetic acid (#A38-212, Thermo Fisher Scientific) and 2.5% (tridecafluoro-1,1,2,2-tetrahydrooctyl)trichlorosilane (#SIT8174, Gelest Inc.) in hexane (#H292, Thermo Fisher Scientific). An additional slide was used to provide a base, with three glass coverslips creating a spacer that held the solution apart to yield a flat gel with a standardized thickness. After polymerization (~10 minutes), the gels were soaked in PBS for at least one hour before functionalization.

Gels were functionalized by UV-photoactivation of a heterobifunctional cross linker, sulfo-SANPAH (#13414, CovaChem), followed by overnight incubation at 4° C in 100 μg/ml solution of collagen type 1 (COL-1, #08-115, Lot #2373345, Millipore).[34] Prior to cell seeding, the gels are washed twice with sterile water and incubated for 10 minutes in 100% ethanol for sterilization. Gels were then rinsed and allowed to equilibrate in base medium, MEM, prior to seeding cells.

Atomic Force Microscopy

Mechanical Characterization of Cells—Non-transfected and transfected WI-38 cells were mechanically characterized using AFM to characterize differences in mechanophenotype. Briefly, single-cell elastic and viscoelastic tests were performed using an AFM based on our previously published techniques, with minor modifications.[7,8,15] Four mechanical parameters were quantified using AFM: elastic modulus ($E_{elastic}$), instantaneous modulus (E_0), relaxed modulus (E_R), and apparent viscosity (μ). $E_{elastic}$ is the measure of a cell's resistance to deformation; a more compliant cell has a lower $E_{elastic}$. E_0 is the initial resistance to deformation, and E_R denotes the stiffness of the cell at equilibrium. Lastly, μ represents the resistance to flow of a cell when a specific stress is applied. Spherically tipped cantilevers were made by adhering 5 μm borosilicate beads to the end of silicon nitride, triangular cantilevers (Bruker Corporation, MLCT-O10, k~0.03 N/m). The AFM was calibrated prior to each experiment by calculating cantilever spring constants based on the power spectral density of the thermal noise fluctuations. Indentation and stress relaxation tests were performed on the perinuclear region of single cells or the center of cell aggregates, with an approach velocity of 10 μm/sec and a 30 second relaxation period. Trigger forces ranged between 0.6 – 1.5 nN to limit indentations to <15% strain based on the height of the cell. All AFM testing was performed at room temperature. Cell and nodule/plaque heights were determined by using the AFM to measure the difference in initial contact location of the cell compared to a reference contact location on the substrate.

Three, separate experiments were performed to characterize the mechanophenotype of transfected and non-transfected cells. The first experiment investigated whether mechanophenotype would change over time on a compliant gel. Non-transfected WI-38 cells were grown on COL-1-coated coverslips and PAAm gels for 5 days. Cells were tested on Day 0 in a spherical morphology (~30 minutes after seeding) and after 1, 2, 3, and 4 days in the nodule/plaque assemblies that formed. The second experiment investigated differences in mechanical properties among GFP-, dnRhoA-, and β-Actin-transfected WI-38 cells. Cells were allowed to adhere to a glass coverslip for 48 hours prior to elastic and viscoelastic testing to determine their mechanophenotype in a spread morphology. The third experiment investigated mechanophenotype and assembly behavior of the mechanically distinct cell types when grown on compliant PAAm gels tuned to precise elasticities. GFP, dnRhoA, and β-Actin cells and cell assemblies grown on COL-1-coated gels or coverslips were mechanically characterized 96 hours after plating. Number of samples tested for each experiment are shown in Supplementary Table 1.

Mechanical Characterization of PAAm Gels—Gels were also characterized using AFM. Briefly, a 4×4 array of indentation sites in 3 distinct locations, for 3 gels per stiffness were collected. As described above, spherically tipped cantilevers were used to indent gel substrates with an indentation rate of 10 μm/sec. The resulting force-indentation curves were fit to the Hertz contact model for spherical indentation of a flat surface. Trigger forces ranged between 1.0 and 1.75 nN to maintain indentations ranging from 0.5 to 1.5 μm.

Confirmation of Transfections Using Western Blot

Protein levels of GFP, dnRhoA, and β-Actin were assessed using Western Blot, following previously described protocols.[27] Briefly, 5 μg of protein were separated on pre-cast SDS-PAGE gels (Bio-Rad) and transferred onto Immobilon IP membranes (Millipore) before probing for GFP (1:2500, Abcam, #ab6556), RhoA (1:500, #MA1-134, Thermo Fisher Scientific), β-Actin (1:2500, #ab170325, Abcam), and GAPDH (1:50,000, #PA1-9046, Thermo Fisher Scientific). Primary antibodies were detected using IRDye 800CW goat anti-mouse (#925-332210), IRDye 680RD donkey anti-rabbit (#925-68073), or IRDye 800CW donkey anti-goat (#926-32214) secondary antibodies (1:15,000, LI-COR). Blots were visualized on an Odyssey Infrared Imaging System (LI-COR). Blots were stripped with NewBlot PVDF Stripping Buffer (LI-COR) and reprobed once to allow for detection of all four proteins on the same blot.

Assessment of Actin Organization and Cellular Assembly

Transfected WI-38 cells were seeded on the three fabricated PAAm gels at a density of 20,000 cells/gel within a 24 well plate (1 gel/well). Three, separate iterations of the experiment were run, with a total of 7–8 gels per condition. After 96 hours of culture, the cells were fixed with 10% formalin, permeabilized with a 0.1% solution of Triton X-100, and blocked with 3% bovine serum albumin. Cells were then stained with phalloidin (#A22287, Molecular Probes, Thermo Fisher) for actin filaments and 4′,6-diamino-2-phenylindole (DAPI, Thermo Fisher) for nuclei. Nine to sixteen images were captured per gel using a 10x objective on the Cytation 3 cell imager (Biotek Instruments Inc.), and cellular assembly was described as either multi-cellular nodules/plaques or single cells/

monolayers (Fig. 1a). Nodule frequency was quantified per field of view (FOV) as a function of cell and gel stiffness using a custom ImageJ (NIH) macro and confirmed by hand counting. Brightness and contrast were uniformly adjusted across entire images to show morphology. Confocal imaging of cellular organization was performed using a Zeiss LSM 510 Meta Confocal Laser Scanning Microscope built on an Axiovert 200M inverted microscope with ZEN 2 software (Carl Zeiss MicroImaging). All images were taken using the 40x objective with 1.05 μm slices. DAPI was visualized using a 405-nm diode laser, and phalloidin was visualized with a 633-nm Helium-Neon laser.

Statistical Analysis

All statistical analysis was performed using SigmaPlot 12.5 (Systat Software Inc.). All data are represented as arithmetic mean ± standard deviation (SD). Cellular mechanical and height data collected using AFM were non-normal, according to the Shapiro-Wilk test. Non-parametric analysis was performed on all data using a Kruskal-Wallis analysis of variance (ANOVA) on ranks, followed by Dunn's test for multiple comparisons with a significance of $p < 0.05$. Nodule frequency data were normalized by logarithmic transform. Significant differences between cell type and PAAm gel stiffness were assessed using a two-factor ANOVA, followed by a Holm-Sidak post-hoc test for multiple comparisons using significance of $p < 0.05$.

Results

Elastic Properties of PAAm Gels

COL-1-coated PAAm gels were fabricated to exhibit elasticities lower, equal to, or greater than those exhibited by transfected WI-38 cells (0.47 ± 0.21 kPa). Resultant gels exhibited elastic moduli of 0.3 ± 0.02 kPa, 0.5 ± 0.04 kPa, and 1.4 ± 0.1 kPa, as measured by AFM.

Temporal Mechanophenotype Characterization of WI-38 Cells

To determine if there was a time component involved in defining cellular mechanophenotype, mechanical properties of non-transfected WI-38 cells were measured across four days while cultured on 0.3, 0.5, and 1.4 kPa gels and glass coverslips (CS). Four parameters, $E_{elastic}$, E_R, E_0, and μ, were measured to obtain a panel of elastic and viscoelastic properties for individual cells exhibiting a spherical morphology on Day 0 (about 30 minutes after seeding) or assemblies of cells in nodule (defined as multi-cellular aggregates) or plaque (defined as flattened versions of nodules) morphologies from Days 1–4 (Fig. 1). Individual cells on glass CS were also tested over the same period. Average $E_{elastic}$ increased from ~0.2 kPa to ~0.5 kPa between Day 0 and Days 1–4 (Fig. 1a). From Days 1–4, cells and nodules/plaques typically exhibited $E_{elastic}$ ranging from 0.4–0.6 kPa, regardless of cellular assembly or substrate stiffness ($p > 0.05$). As with the elastic modulus, E_R, E_0, and μ varied on Day 0 based on substrate stiffness but stabilized to a consistent, stiffer mechanophenotype on Days 1–4 ($p > 0.05$, Fig. 1b–d). In general, WI-38 cells in nodule formation on 0.3 and 0.5 kPa gels were significantly taller than their corresponding plaques formed on 1.4 kPa gels for each day (Supplementary Fig. 1). Individual WI-38 cells on glass CS were significantly shorter than nodules or plaques on gels.

Transfection and Mechanical Characterization of WI-38 Cells

Successful transfections of WI-38 cells with GFP, dnRhoA, or β-Actin plasmids were visualized by green fluorescence from the GFP reporter (Fig. 2a). Western blots confirmed successful incorporation of plasmid DNA and subsequent expression of GFP-fused proteins based on the presence of higher molecular weight bands for all modified groups (Fig. 2b). $E_{elastic}$ of the three transfected cell lines was mechanically characterized after two days on glass coverslips using AFM (Fig. 2c). β-Actin cells were ~30% more compliant than GFP cells ($p < 0.05$), while dnRhoA cells were ~60% stiffer ($p < 0.05$). dnRhoA cells were ~130% stiffer than β-Actin cells ($p < 0.05$).

Effect of Mechanophenotype on Cellular Organization

Two, distinct, organizational phenotypes, multi-cellular nodules/plaques versus single cells/monolayers, were visible across all cell lines and across gels regardless of their stiffness. DAPI and phalloidin staining provided more detail on these particular cell arrangements (Fig. 3). Qualitatively, GFP and dnRhoA cells primarily formed nodules on 0.3 and 0.5 kPa gels, elastic moduli that were equal to or less than that measured for either cell type (Fig. 3a). Interestingly, β-Actin cells displayed the lowest nodule frequency per FOV compared to the other two cell types across all three gel stiffnesses ($p < 0.05$, Fig. 3b). While not statistically significant, β-Actin cells tended to form fewer nodules on the 0.3 kPa gels than either GFP or dnRhoA cells (50–55% fewer, $p = 0.07$ for both comparisons). β-Actin cells also formed significantly fewer nodules than dnRhoA cells on 0.5 kPa (60% fewer, $p = 0.01$) and 1.4 kPa (71% fewer, $p = 0.02$) gels. Similar trends were observed between β-Actin and GFP cells on 0.5 kPa (53% fewer, $p = 0.15$) and 1.4 kPa (62% fewer, $p = 0.13$) gels. For all cell types investigated, nodule frequency on the 1.4 kPa gels was significantly less than on 0.3 and 0.5 kPa gels ($p < 0.05$). Similar observations were made for cell types spanning across other lineages (Supplementary Fig. 2–3).

Mechanophenotype of GFP, dnRhoA, and β-Actin Cells on Compliant Gels

The behavior of mechanically distinct, stably transfected cell lines was then observed when grown on substrates with stiffness above, below, and equal to the elastic modulus of the cell. Mechanical properties of cells from the four cell lines grown on COL-1-coated 0.3, 0.5, 1.4 kPa gels and glass CS were measured at a single time point, Day 4. The mechanophenotype of cells in nodule or plaque morphologies was recorded for each of the cell types. Interestingly, no differences in $E_{elastic}$, E_R, E_0, or μ (Fig. 4a–d) were observed among nodules and plaques formed by GFP, dnRhoA, or β-Actin cells on the gels ($p > 0.05$). Additionally, no differences in mechanical properties were observed between nodules or plaques on gels and individual cells on glass CS (Fig. 4 and electronic supplementary material, table S1c). While the heights of individual cells compared to nodules and plaques varied due to increased cell numbers (Supplementary Fig. 4), this did not affect cellular mechanophenotype.

Confocal Imaging of Actin Cytoskeleton

Confocal z-stacks of DAPI- and phalloidin-stained cells were taken 96 hours after culture on gels of designated stiffness (Fig. 5). Qualitatively, nodules formed by GFP cells on 0.3 kPa

and 0.5 kPa gels showed more centralized actin cytoskeleton that became more diffuse and less visible towards the edges of the nodule. On the 1.4 kPa gel, GFP cells primarily formed plaques that displayed a highly structured network of actin filaments. dnRhoA cells on 0.3 kPa gels displayed minimally structured actin cytoskeleton, instead presenting punctate actin structures throughout the cytoplasm. Similar to GFP cells, dnRhoA on 0.5 and 1.4 kPa gels had a centralized actin cytoskeleton where cells were in contact with other cells and had minimal interaction with the underlying compliant gel. β-Actin cells cultured on 0.3 kPa gels showed diffuse phalloidin staining throughout the cytoplasm and minimal structured cytoskeleton. Conversely, on 0.5 and 1.4 kPa gels, which were stiffer than β-Actin cells, cells displayed organized actin fibers. Unlike other cell types, β-Actin cells were able to adhere to gels as single cells and completely spread out.

Discussion

Results from this study indicate that inherent mechanophenotype influences cellular assembly when grown on substrates exhibiting elasticities similar to the cells themselves. Cells maintained a characteristic, perinuclear, whole-cell mechanophenotype on all substrates, regardless of their stiffness, and across all group morphologies and assemblies formed by the cells. Non-transfected WI-38 cells reached a stable mechanical state one day after plating and maintained this mechanophenotype throughout the remaining three days of the experiment. Mechanically distinct GFP-, dnRhoA-, and β-Actin-transfected cells also displayed inherent, whole-cell mechanical signatures that appeared to be largely decoupled from the external microenvironment. Additionally, the results from this study indicate that cells have the ability to mechanosense their environment and selectively adhere and spread on whatever material, PAAm substrate or neighboring cells, that is stiffer than their inherent mechanophenotype. The most compliant cell type in the study exhibited the least amount of nodule formation across all three gels, suggesting a preference to adhere to the stiffer substrate than soft, neighboring cells. Furthermore, for all cell types, significantly greater nodule formation was observed on 0.3 and 0.5 kPa PAAm gels compared to 1.4 kPa gels, where cells were able to spread and develop a more structured actin cytoskeleton.

The inherent mechanophenotype of WI-38 cells varied during initial attachment to a substrate but remained largely stable over time. The different cellular assemblies observed throughout the study also formed within the first day, indicating that cells could react quickly to their microenvironment. Since the mechanical properties of WI-38 cells did not change over time, comparisons among the transfected cell lines were made at a single time point. Mechanically distinct, transfected WI-38 cell lines also maintained their inherent, whole-cell mechanophenotypes on substrates of varying stiffness. These results are supported by other studies that have also observed a stable, inherent mechanophenotype despite changes to the cellular microenvironment. Poh et al. showed that embryonic stem cells did not increase their apical cell stiffness on substrates of varying stiffness, while basal traction forces did increase at the interface of cell-substrate interactions on PAAm gels ranging from 0.35 to 8 kPa.[25] Jagielska et al. observed that oligodendrocyte progenitor cells were more compliant than differentiated oligodendrocytes. However, both progenitor and differentiated cell stiffnesses were independent of PAAm gel elasticity, ranging from 0.1 to 70 kPa.[18] It is important to note that Jagielska's study observed changes in cell survival,

proliferation, migration, and other biological factors that were independent of cellular mechanophenotype, emphasizing that this parameter is not solely a secondary indicator of normal cell functions.[18] Contrary to our results, other studies have suggested that mechanophenotype is a more malleable characteristic that changes to match the elasticity of whatever surface the cell is attached to.[18,25,29–31] However, these experiments differ substantially in the mechanical testing techniques used (AFM using sharp pyramidal tips over the cytoplasm/cytoskeleton rather than spherical beads over the perinuclear region), range of PAAm gel stiffness examined (0.5 – 40 kPa, many-fold higher than WI-38 mechanophenotype), and cell type investigated (e.g., fibroblasts vs. glioma cells vs. endothelial cells). The current study focused on whole-cell properties to provide an average measure of mechanical properties associated with a cell, rather than nanometer-sized, point tests that can vary widely depending on what underlying cellular component is contacted. Gel elasticity was also limited to only those stiffnesses immediately higher and lower to the cells used in the work, rather than including elasticities orders of magnitude greater. In this way, the work narrowly focuses on studying competitive adherence, due to elasticity, of cells on a soft surface.

This study identified that mechanophenotype plays a role in cellular assembly on mechanically-varied substrates, which could be a key factor to consider in tissue formation and development. A clear transition in organizational phenotype was observed across all three WI-38-transfected cell lines tested. GFP ($E_{elastic}$ ~ 0.55 kPa), and dnRhoA ($E_{elastic}$ ~ 0.87 kPa) cell lines exhibited significantly more nodule formation on 0.3 kPa and 0.5 kPa gels, with cells preferentially adhering to each other over the softer gel. Comparatively, β-Actin cells ($E_{elastic}$ ~ 0.37 kPa) readily adhered and spread on the softer gels, even maintaining single-cell morphologies rather than multi-cell assemblies. These findings confirmed our hypothesis that cells would competitively bind with the stiffest substrate they sense, whether that is a surface or neighboring cell.

Confocal imaging provided further insight into the differences in the actin cytoskeleton network developed in the various types of cellular assemblies. The integrated cytoskeletal network that existed across multiple cells can form through cadherins in cell-cell adhesions, which facilitate cell layers and assemblies within tissues and are the adhesive mechanism for tissue-specific structures.[4,36] Cadherins also direct actin assembly through coupling proteins, such as β-catenin, α-catenin, and vinculin.[36] Previous studies with similar observations in cellular assembly attribute this behavior to cells maximizing their mechanical input from the microenvironment.[16] Gilchrist et al. observed nucleus pulposus cells ($E_{elastic}$ ~0.35 ± 0.20 kPa) preferred to aggregate (the typical cellular arrangement *in vivo*) on 0.10 and 0.22 kPa PAAm gels, yet spread out and form an ordered actin cytoskeleton on 0.72 kPa gels.[14] These phenomena may be explained by differences in expression of Rho pathway components and their link to myosin-II associated contractility.[16] These proteins help cells sense their environment by regulating formation of focal adhesions (integrins) and by mediating cell-cell interactions (cadherins). Therefore, cellular mechanophenotype, in combination with substrate compliance, can influence mechanosensing of the microenvironment and, ultimately, tissue formation.

This study strived to create a controlled system to test the effect of mechanophenotype on the various cellular assemblies by creating stable cell lines. These stable transfections minimized variation due to genetic differences and provided a more consistent phenotype compared to commonly used pharmacologic treatments, such as cytochlasin D (inhibitor of actin polymerization), blebbistatin (myosin II inhibitor), or Y-27632 (ROCK inhibitor). By transfecting a common background cell type with cytoskeleton-related genes, dnRhoA or β-Actin, two mechanically distinct cell lines were developed, with a GFP-transfected cell line serving as a control. Transfection with the dominant negative RhoA (point mutation T19N) created the stiffest cell type, while transfection with β-Actin created the most compliant cell type. While there were visible changes in morphologies of these two cell types, their changes in mechanical properties were contrary to what would be expected. dnRhoA cells were transfected with a mutated, non-functional version of RhoA that inhibits activation of Rho kinase and downstream actin assembly but displayed typical cell spreading behaviors, as observed previously.[13] In the current work, dnRhoA-GFP-transfected cells maintained their endogenous RhoA (as identified by western blot expression levels), in addition to the mutated RhoA, with mechanophenotype stiffening as a response. β-Actin-transfected cells visibly incorporated β-Actin-GFP into their actin fibers; however, much diffuse, β-Actin remained in the cytoplasm as well. While previous studies indicate a ~5–10% increase in overall actin expression is to be expected, a corresponding increase in whole-cell stiffness was not observed in the current study.[5,10] To our knowledge, researchers using the dnRhoA-GFP or β-Actin-GFP transfections have only investigated changes in cell morphology, differentiation potential, actin organization, and protein content, while whole-cell mechanical properties were not assessed.[5,10,13,22] While the mechanisms behind gene-specific mechanophenotype responses are not within the scope of this study, we hypothesize the apparent contradiction may be due to alternative feedback mechanisms through components of the Rho pathway. The activation of Rho kinase may occur through secondary mechanisms (instead of by RhoA), which would lead to continued stabilization of actin, development of stress fibers, and whole-cell stiffening.[2] Comparatively, while overexpression of β-Actin leads to increased monomeric actin (visualized by the diffuse green fluorescence in the cytoplasm, Fig. 2a), this may not be completely translated into filamentous F-actin that makes up stress fibers and correlates with cell stiffness. Additionally, the β-Actin-GFP fusion protein has been shown to inhibit various actin binding proteins and myosin-II interactions in protozoa which could lead to dysfunction of the actin structure, and thus, a more compliant cell.[1,17]

While the current study used COL-1 as a substrate coating for all conditions, it is likely that ECM ligands will play an important role in cellular assembly by restricting integrin binding for cell types of more varied backgrounds. Supplementary experiments explored this hypothesis by investigating how cells from multiple lineages responded to fibronectin (FN) and laminin (LN), in addition to COL-1. MG-63 (osteosarcoma, $E_{elastic}$ = 1.3 ± 0.5 kPa) and SH-SY5Y (neuroblastoma, $E_{elastic}$ = 0.3 ± 0.1 kPa) cells were grown on PAAm gels coated in the different proteins. While a ligand-dependent adhesion response was observed (Supplementary Fig. 2), cellular mechanophenotype was still maintained across gels (Supplementary Fig. 3). Protein coatings had a modulatory effect on cellular mechanosensing as well, likely due to disparate integrin binding interactions. MG-63 cells

spread more on COL-1, even on soft gels. Highly compliant SH-SY5Y cells spread and exhibited the same morphologies on all three gel stiffnesses, which were greater than or equal to the ~0.3 kPa elastic modulus of SH-SY5Y cells. Notably, binding affinity was weak on soft, LN- and FN-coated gels. Additionally, SH-SY5Y cell morphologies are inherently cell density dependent, aggregating when seeded at lower cell densities or spreading and forming monolayers at higher densities (Supplementary Fig. 2b, c).[26] These results suggest that inherent mechanophenotype influences cellular assembly across multiple types of cells, but are only one factor since other environmental conditions like protein ligands can exert influences of their own.

Single-cell mechanical properties exhibit large variations. If biological phenotype is not a concern, cell populations can be chosen that are mechanically distinct (e.g., MG-63 and SH-SY5Y). While stable transfections of a common background cell type created mechanically distinct cell populations in the current study, the induced stiffening or softening were not extensive enough to completely separate their mechanophenotype distributions. Therefore, cell assembly responses on the various substrates were more heterogeneous. Cells exhibiting a “soft” mechanophenotype were inevitably present in small proportions in the “stiffer” cell type groups and vice versa. Regardless, sufficient separation in average mechanophenotype was achieved to discern generalized cell assembly behaviors. Complete knockdown of genes, promoters, or modulation of other elements that have a more dramatic effect on the whole-cell properties may provide even clearer evidence of what is reported here.

Whole-cell mechanophenotype affects critical functions, including proliferation, differentiation, motility, shape, and multi-cell assembly.[9] Therefore, understanding how mechanophenotype influences cell behavior in relation to the local, mechanical microenvironment is vital to directing successful cellular organization in regenerating tissues. The ability of cells to aggregate or spread individually depends not only on cell type, extracellular matrix ligands, and substrate stiffness, but also importantly on inherent mechanophenotype.[14,37] These findings can provide insight into future studies on tissue engineered constructs as well as the pathological progression of injuries and disease based on combined data from mechanical changes in extracellular matrix and cellular properties.

Supplementary Material

Refer to Web version on PubMed Central for supplementary material.

Acknowledgments

The authors would like to thank Louise E. O. Darling for the GFP plasmids and Jessica S. Sadick and Vera Fonseca for help with western blots. This work was supported by awards from the National Institute of Health (R01 AR063642, P20 GM104937) and the National Science Foundation (CAREER CBET 1253189). The content of this article is solely the responsibility of the authors and does not necessarily represent the official views of the National Science Foundation or National Institutes of Health

Abbreviations, symbols, terminology

AFM	atomic force microscopy
COL-I	collagen type-1

dnRhoA	dnRhoA (T19N) - GFP transfected WI-38 cells
ECM	extracellular matrix
$E_{elastic}$	elastic modulus
E_0	instantaneous modulus
E_R	relaxed modulus
FN	fibronectin
LN	laminin
PAAm	polyacrylamide
WI-38	WI-38 VA-13 subline 2RA
β-Actin	β-Actin-GFP transfected WI-38 cells
μ	apparent viscosity

References

1. Aizawa H, Sameshima M, Yahara I. A green fluorescent protein-actin fusion protein dominantly inhibits cytokinesis, cell spreading, and locomotion in Dictyostelium. Cell Struct Funct. 1997; 22(3):335–45. [PubMed: 9248997]
2. Amin E, Dubey BN, Zhang SC, Gremer L, Dvorsky R, Moll JM, Taha MS, Nagel-Steger L, Piekorz RP, Somlyo AV, Ahmadian MR. Rho-kinase: regulation, (dys)function, and inhibition. Biol Chem. 2013; 394(11):1399–410. [PubMed: 23950574]
3. Brafman DA. Constructing stem cell microenvironments using bioengineering approaches. Physiol Genomics. 2013; 45(23):1123–35. [PubMed: 24064536]
4. Brieher WM, Yap AS. Cadherin junctions and their cytoskeleton(s). Current Opinion in Cell Biology. 2013; 25(1):39–46. [PubMed: 23127608]
5. Choidas A, Jungbluth A, Sechi A, Murphy J, Ullrich A, Marriott G. The suitability and application of a GFP-actin fusion protein for long-term imaging of the organization and dynamics of the cytoskeleton in mammalian cells. Eur J Cell Biol. 1998; 77(2):81–90. [PubMed: 9840457]
6. Darling EM, Di Carlo D. High-Throughput Assessment of Cellular Mechanical Properties. Annu Rev Biomed Eng. 2015
7. Darling EM, Topel M, Zauscher S, Vail TP, Guilak F. Viscoelastic properties of human mesenchymally-derived stem cells and primary osteoblasts, chondrocytes, and adipocytes. J Biomech. 2008; 41(2):454–64. [PubMed: 17825308]
8. Darling EM, Zauscher S, Block JA, Guilak F. A thin-layer model for viscoelastic, stress-relaxation testing of cells using atomic force microscopy: do cell properties reflect metastatic potential? Biophys J. 2007; 92(5):1784–91. [PubMed: 17158567]
9. Di Carlo D. A Mechanical Biomarker of Cell State in Medicine. Jala. 2012; 17(1):32–42. [PubMed: 22357606]
10. Engler A, Bacakova L, Newman C, Hategan A, Griffin M, Discher D. Substrate compliance versus ligand density in cell on gel responses. Biophys J. 2004; 86(1 Pt 1):617–28. [PubMed: 14695306]
11. Engler AJ, Sen S, Sweeney HL, Discher DE. Matrix elasticity directs stem cell lineage specification. Cell. 2006; 126(4):677–89. [PubMed: 16923388]
12. Georges PC, Janmey PA. Cell type-specific response to growth on soft materials. J Appl Physiol (1985). 2005; 98(4):1547–53. [PubMed: 15772065]

13. Ghosh PM, Ghosh-Choudhury N, Moyer ML, Mott GE, Thomas CA, Foster BA, Greenberg NM, Kreisberg JI. Role of RhoA activation in the growth and morphology of a murine prostate tumor cell line. Oncogene. 1999; 18(28):4120–4130. [PubMed: 10435593]
14. Gilchrist CL, Darling EM, Chen J, Setton LA. Extracellular Matrix Ligand and Stiffness Modulate Immature Nucleus Pulposus Cell-Cell Interactions. Plos One. 2011; 6(11)
15. Gonzalez-Cruz RD, Fonseca VC, Darling EM. Cellular mechanical properties reflect the differentiation potential of adipose-derived mesenchymal stem cells. Proc Natl Acad Sci U S A. 2012; 109(24):E1523–9. [PubMed: 22615348]
16. Guo WH, Frey MT, Burnham NA, Wang YL. Substrate rigidity regulates the formation and maintenance of tissues. Biophys J. 2006; 90(6):2213–20. [PubMed: 16387786]
17. Hosein RE, Williams SA, Haye K, Gavin RH. Expression of GFP-actin leads to failure of nuclear elongation and cytokinesis in Tetrahymena thermophila. J Eukaryot Microbiol. 2003; 50(6):403–8. [PubMed: 14733431]
18. Jagielska A, Norman AL, Whyte G, Vliet KJ, Guck J, Franklin RJ. Mechanical environment modulates biological properties of oligodendrocyte progenitor cells. Stem Cells Dev. 2012; 21(16): 2905–14. [PubMed: 22646081]
19. Kular JK, Basu S, Sharma RI. The extracellular matrix: Structure, composition, age-related differences, tools for analysis and applications for tissue engineering. J Tissue Eng. 2014; 5 2041731414557112.
20. Labriola NR, Darling EM. Temporal heterogeneity in single-cell gene expression and mechanical properties during adipogenic differentiation. Journal of Biomechanics. 2015; 48(6):1058–1066. [PubMed: 25683518]
21. Lo CM, Wang HB, Dembo M, Wang YL. Cell movement is guided by the rigidity of the substrate. Biophysical Journal. 2000; 79(1):144–152. [PubMed: 10866943]
22. McBeath R, Pirone DM, Nelson CM, Bhadriraju K, Chen CS. Cell shape, cytoskeletal tension, and RhoA regulate stem cell lineage commitment. Dev Cell. 2004; 6(4):483–95. [PubMed: 15068789]
23. Mendez MG, Restle D, Janmey PA. Vimentin Enhances Cell Elastic Behavior and Protects against Compressive Stress. Biophysical Journal. 2014; 107(2):314–323. [PubMed: 25028873]
24. Parsons JT, Horwitz AR, Schwartz MA. Cell adhesion: integrating cytoskeletal dynamics and cellular tension. Nat Rev Mol Cell Biol. 2010; 11(9):633–43. [PubMed: 20729930]
25. Poh YC, Chowdhury F, Tanaka TS, Wang N. Embryonic stem cells do not stiffen on rigid substrates. Biophys J. 2010; 99(2):L19–21. [PubMed: 20643049]
26. Ross RA, Spengler BA, Biedler JL. Coordinate Morphological and Biochemical Interconversion of Human Neuro-Blastoma Cells. Journal of the National Cancer Institute. 1983; 71(4):741–749. [PubMed: 6137586]
27. Sadick JS, Boutin ME, Hoffman-Kim D, Darling EM. Protein characterization of intracellular target-sorted, formalin-fixed cell subpopulations. Sci Rep. 2016; 6:33999. [PubMed: 27666089]
28. Schwarz US, Gardel ML. United we stand: integrating the actin cytoskeleton and cell-matrix adhesions in cellular mechanotransduction. J Cell Sci. 2012; 125(Pt 13):3051–60. [PubMed: 22797913]
29. Sen S, Dong M, Kumar S. Isoform-specific contributions of alpha-actinin to glioma cell mechanobiology. PLoS One. 2009; 4(12):e8427. [PubMed: 20037648]
30. Sen S, Ng WP, Kumar S. Contributions of talin-1 to glioma cell-matrix tensional homeostasis. J R Soc Interface. 2012; 9(71):1311–7. [PubMed: 22158841]
31. Solon J, Levental I, Sengupta K, Georges PC, Janmey PA. Fibroblast adaptation and stiffness matching to soft elastic substrates. Biophys J. 2007; 93(12):4453–61. [PubMed: 18045965]
32. Stroka KM. Aranda-Espinoza HEffects of Morphology vs. Cell-Cell Interactions on Endothelial Cell Stiffness. Cellular and Molecular Bioengineering. 2011; 4(1):9–27. [PubMed: 21359128]
33. Suresh S. Biomechanics and biophysics of cancer cells. Acta Biomater. 2007; 3(4):413–38. [PubMed: 17540628]
34. Tse JR, Engler AJ. Preparation of hydrogel substrates with tunable mechanical properties. Curr Protoc Cell Biol. 2010; Chapter 10(Unit 10):16.

35. Wang JH, Lin JS. Cell traction force and measurement methods. Biomech Model Mechanobiol. 2007; 6(6):361–71. [PubMed: 17203315]

36. Weber GF, Bjerke MA, DeSimone DW. Integrins and cadherins join forces to form adhesive networks. J Cell Sci. 2011; 124(Pt 8):1183–93. [PubMed: 21444749]

37. Yeung T, Georges PC, Flanagan LA, Marg B, Ortiz M, Funaki M, Zahir N, Ming W, Weaver V, Janmey PA. Effects of substrate stiffness on cell morphology, cytoskeletal structure, and adhesion. Cell Motil Cytoskeleton. 2005; 60(1):24–34. [PubMed: 15573414]

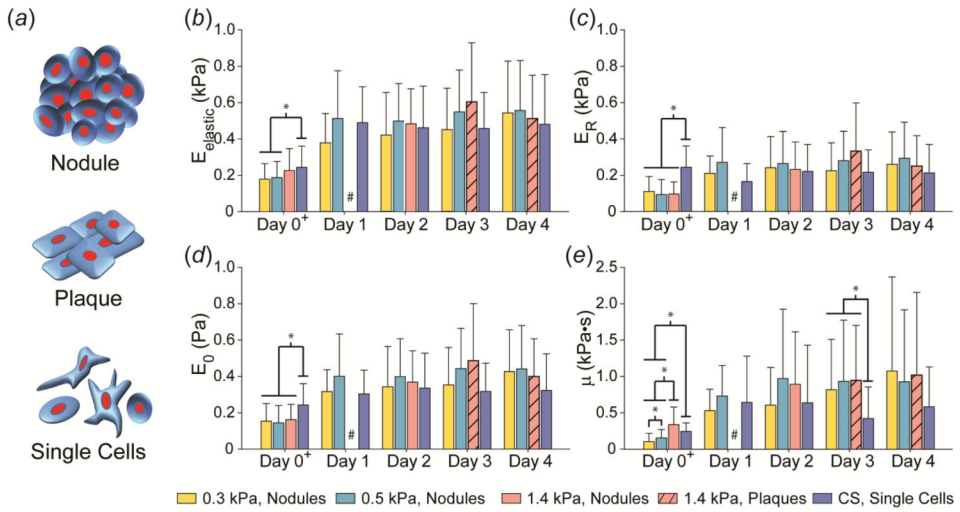

Figure 1.

Mechanical characterization of the cellular assemblies formed by WI-38 cells on compliant substrates over 5 days. (a) Different cellular assemblies formed when cells were cultured on compliant gels. Nodules represent three-dimensional cellular aggregates. Plaques represent a flattened version of the nodules. And lastly, single cells represent a variety of morphologies demonstrated by non-assembling cells, present at early time points for all substrates and at later time points on substrates with elasticities stiffer than the mechanophenotype of the cell. Average mechanical properties, (b) $E_{elastic}$, (c) E_R, (d) E_0, and (e) μ, of single and assembled WI-38 cells over four days across PAAm gels and glass coverslips (CS). In general, cells tested on Day 0, about 30 minutes after seeding, showed the most variation due to substrate stiffness for all four mechanical properties. WI-38 cells maintained their mechanophenotype from Day 1 onwards, regardless of organizational morphology and substrate stiffness. At later time points, cells only formed plaques on the 1.4 kPa gel, which exhibited mechanical properties similar to the nodules formed on other gels and single cells on glass CS. Data shown as mean ± s.d., with statistical significance determined using Kruskal-Wallis ANOVA on ranks within each day, followed by a Dunn's post-hoc analysis (* $p < 0.05$). #, Only single cells were present for this condition, instead of nodules/plaques. +, Individual cells in spherical morphologies were tested on Day 0 for all substrates.

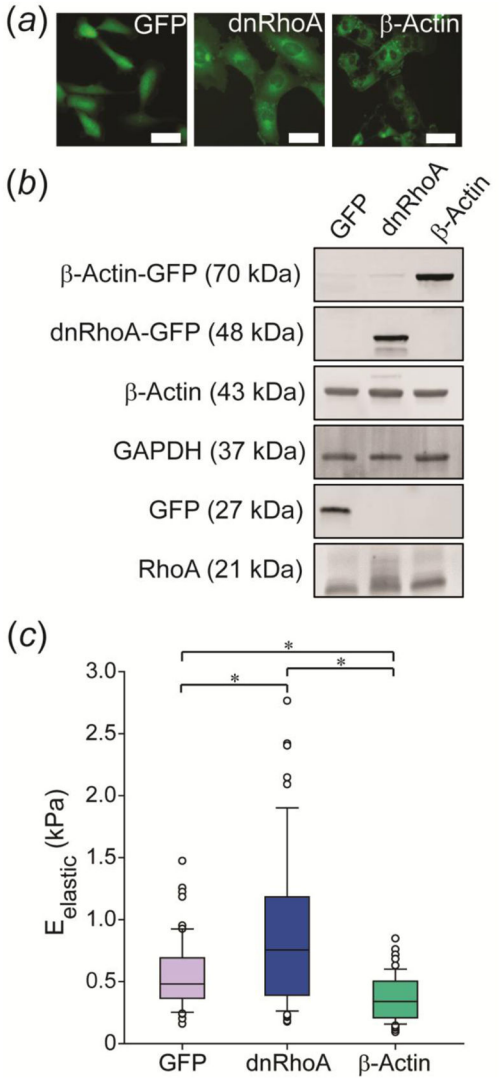

Figure 2.

Characterization of GFP, dnRhoA, and β-Actin cells. (a) Stably transfected cell lines exhibited uniform GFP expression. Scale bar = 50 μm. (b) Expression of fusion proteins was confirmed via Western blot analysis. (c) Each cell line was mechanically characterized when adhered to glass coverslips for two days, with results showing higher (dnRhoA) and lower (β-actin) elastic moduli in comparison to the control, GFP-transfected cells. Data shown as mean ± s.d., with statistical significance determined using Kruskal-Wallis ANOVA on ranks, followed by a Dunn's post-hoc analysis (* $p < 0.05$).

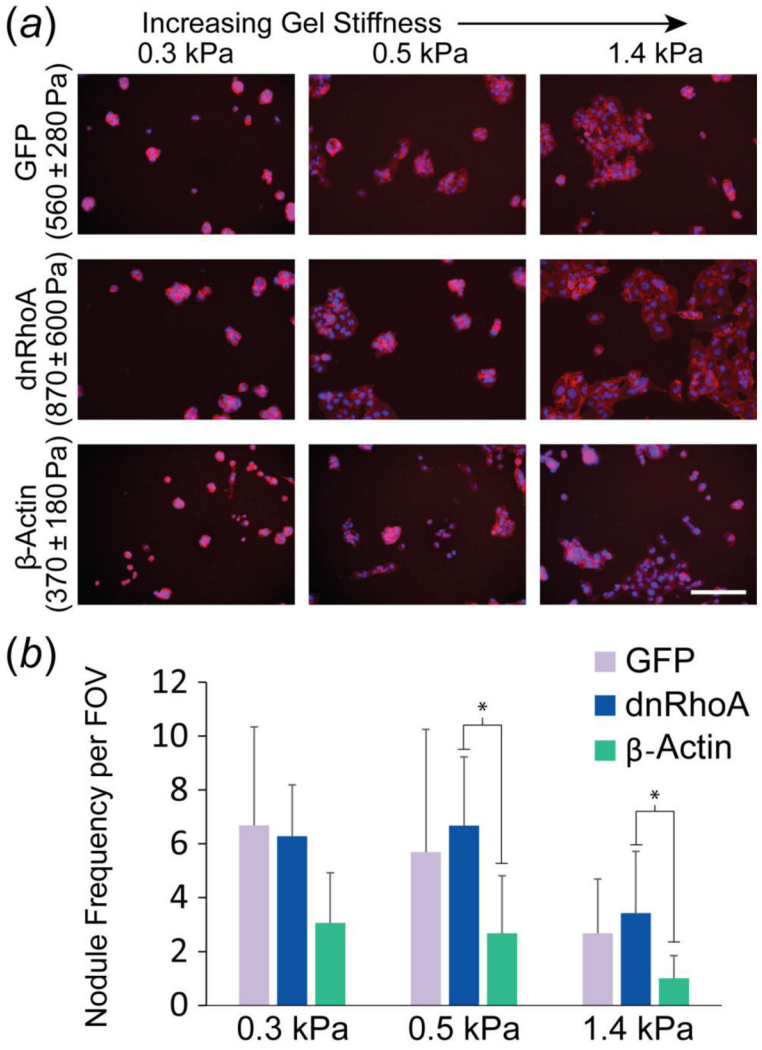

Figure 3.

Effect of mechanophenotype on cellular assembly into nodules or plaques. (a) Representative images of transfected WI-38 cells on PAAm gels (nuclei: *blue*, actin filaments: *red*; scale bar: 200 μm). (b) Abundant nodule formation occurred on gels that were more compliant than the inherent mechanophenotype of cells in the noted cell line. Nodule frequency per field of view (FOV) shown as mean ± s.d. (* $p < 0.05$, as determined by a two-factor ANOVA between cell type and gel stiffness on logarithmically transformed data, followed by Holm-Sidak post-hoc analysis).

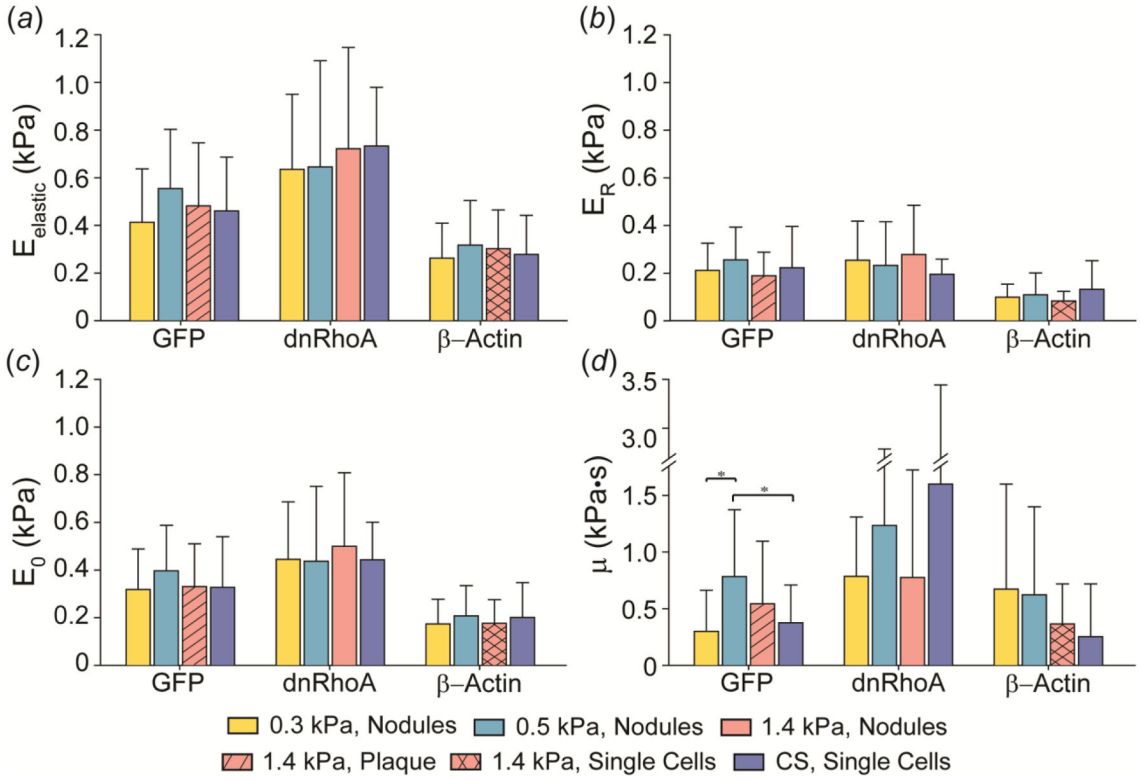

Figure 4.

Average mechanical properties, (a) $E_{elastic}$, (b) E_R, (c) E_0, and (d) μ, of GFP-, dnRhoA-, and β-Actin-transfected WI-38 cells after four days on 0.3, 0.5, and 1.4 kPa PAAm gels and glass coverslips (CS). In general, cells displayed similar mechanical properties, regardless of organizational morphology (nodule vs. plaque vs. single cells) and substrate stiffness. Data shown as mean ± s.d., with statistical significance determined using Kruskal-Wallis ANOVA on ranks for each mechanical parameter within each cell line, followed by a Dunn's post-hoc analysis (* $p < 0.05$).

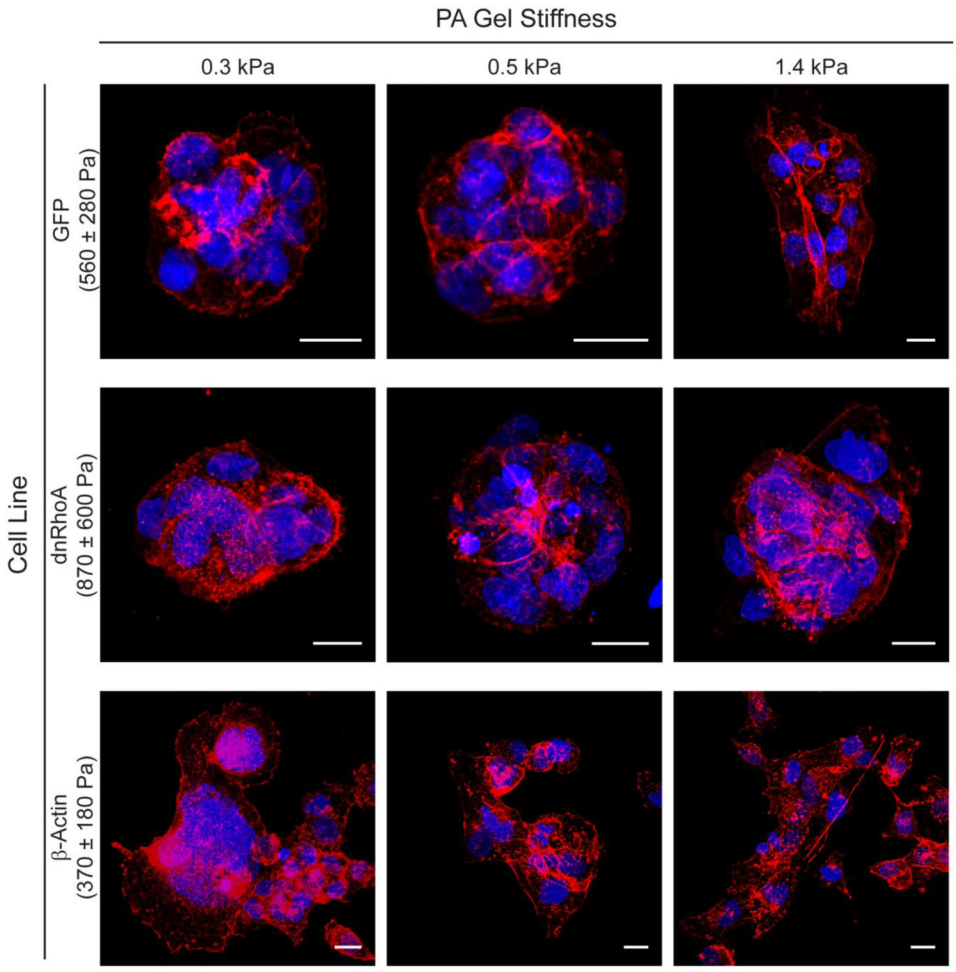

Figure 5.

Nodules and plaques of GFP, dnRhoA, and β-Actin cells after 4 days of culture. Confocal projections revealed differences in actin bundle formation (nuclei: *blue*, actin filaments: *red*; scale bars: 20 μm) on gels, especially as cells transitioned from nodule to plaque formations on PAAm gels greater than the mechanophenotype of the adhered cells.